

Back Reaction from Walls

Enea Di Dio

*Département de Physique Théorique and Center for Astroparticle Physics,
Université de Genève,
24 quai Ernest Ansermet, CH-1211 Genève 4, Switzerland
enea.didio@unige.ch*

Marc Vonlanthen

*Département de Physique Théorique and Center for Astroparticle Physics,
Université de Genève,
24 quai Ernest Ansermet, CH-1211 Genève 4, Switzerland
marc.vonlanthen@unige.ch*

Ruth Durrer

*Département de Physique Théorique and Center for Astroparticle Physics,
Université de Genève,
24 quai Ernest Ansermet, CH-1211 Genève 4, Switzerland
ruth.durrer@unige.ch*

ABSTRACT: We study the distance–redshift relation in a universe filled with ‘walls’ of pressure-less dust separated by under dense regions. We show that as long as the density contrast of the walls is small, or the diameter of the under dense regions is much smaller than the Hubble scale, the distance–redshift relation remains close to what is obtained in a Friedmann universe. However, when arbitrary density contrasts are allowed, every prescribed distance–redshift relation can be reproduced with such models.

KEYWORDS: Dark Energy, Back Reaction, Plane Symmetry.

Contents

1. Introduction	1
2. Wall Universes	2
2.1 The solutions	3
2.2 Singularities	5
3. The distance redshift relation in a wall universe	7
3.1 Generalities	7
3.1.1 Redshift	7
3.1.2 Distance	9
3.2 'Realistic' walls	10
3.3 Mimicking dark energy	13
3.4 Redshift drift	16
4. Conclusions	18
A. Derivation of the system of differential equations and initial conditions	19
A.1 The system	19
A.2 Initial conditions	21
B. Derivation of the system of differential equations for the redshift drift	22
C. The linearized approach	22

1. Introduction

Since more than a decade, cosmology research is facing the dark energy problem: the present Universe seems to be in an accelerating phase. This conclusion was first drawn from measurements of the distance–redshift relation from type Ia Supernovae (SNIa) [1, 2] and is confirmed by many other datasets, from the cosmic microwave background [3] to baryon acoustic oscillations and other aspects of large scale structure. Until very recently the measurements inferring the existence of dark energy rely mainly on the distance–redshift relation which is valid in a Friedmann Universe [4]. New *independent* measurements of, e.g. the expansion rate $H(z)$ are now being performed see e.g. [5]. Hence this situation is changing, so that we shall soon know both, $d_A(z)$ and $H(z)$ with good accuracy. The general opinion is that fluctuations on large scales are small so that they can be treated with linear perturbation theory and linear perturbations average out in the mean over many directions and large scales, and therefore fluctuations are not relevant for the determination

of quantities like $d_A(z)$ and $H(z)$. This expectation has been confirmed by perturbative calculations. Within linear perturbation theory, the fluctuations of the distance–redshift relation for redshift $z > 0.2$ is on the level of a few percent [6].

However, perturbations on smaller scales can become very large, density fluctuations e.g. in galaxies are $\delta\rho/\rho \sim \rho_{\text{gal}}/\rho_m \sim 10^8$. Since the relation between metric perturbations, or more precisely the Christoffel symbols, and density fluctuations is non-linear, it is not evident that large amplitude, non-linear, small scale density fluctuations cannot add up to affect the distance–redshift relation on large scales.

To study the real problem one would need to analyse light rays passing through a realistic Universe with high density fluctuations. So far, this has been done only within Newtonian N-body simulations, see e.g. [7]. However, it is well known that Newtonian gravity misses the terms which are relevant for the back reaction problem [8], hence a full, non-linear relativistic treatment is needed. Since this is very difficult, so far mainly toy models which mimic reality to a certain extent have been studied.

The present work inscribes in this framework. Instead of considering spherically symmetric solutions of general relativity (GR), the so called Lemaître [9]-Tolman [10]-Bondi (LTB) models, for recent reviews see [11], we study a Universe containing high density walls. We shall consider infinitely extended parallel walls. The considered model is a sub-case of the Szekeres solution [12]. Light propagation in general Szekeres model has been studied recently [13, 14]. This is of course a gross over-simplification, but we know that galaxies tend to be aligned in filaments and photons coming to us from a far away supernova, might experience a geometry similar to the one of such a symmetric wall universe. The weakest point of our toy model is that all the walls are parallel while we expect a typical photon to traverse filaments which are aligned in different directions. We shall take this into account to some extent by studying photons coming in from different directions with respect to the walls.

Such walls have been studied in the past [15], but only perturbatively. Since we know that the effects are small within linear perturbation theory, we cannot trust higher order perturbation theory if it predicts large deviations from the Friedmann distance-redshift relation. For this reasons we analyse exact, fully relativistic wall-universes in this work.

In the next section we present the wall metric and the Einstein equations. We also study the conditions on the parameters which have to be satisfied so that no singularity apart from the Big Bang is present in the backward light cone of the observer. In section 3 we present the results for the distance-redshift relation for 'realistic' walls and for a wall universe which mimics the observed relation. In section 4 we conclude.

2. Wall Universes

In this section we study universes containing only pressure-less matter (dust) and which are symmetric under translations and rotations in a plane which we call the y -plane. They have the same number of symmetries as LTB models and can be solved analytically, see [16]. The metric is of the form

$$ds^2 = -dt^2 + a^2(t, x)dx^2 + b^2(t, x)(dy_1^2 + dy_2^2). \quad (2.1)$$

Note that the only difference to the LTB geometry is that our symmetrical 2d manifolds are planes, $dy_1^2 + dy_2^2 = dr^2 + r^2 d\phi^2$ while those of LTB are spheres, $d\Omega^2 = d\theta^2 + \sin^2 \theta d\phi^2$. We denote the spatial coordinates by $\mathbf{x} = (x, y_1, y_2)$ in order to reserve the letter z for the redshift. In the following a prime denotes a derivative w.r.t. x while a dot denotes derivative w.r.t. t . The Einstein equations for this geometry and for pure dust matter yield [12, 16, 17]

$$\partial_t \left(\frac{b'}{a} \right) \equiv \partial_t E = 0, \quad (2.2)$$

$$\dot{b}^2 - \left(\frac{b'}{a} \right)^2 = 2 \frac{M(x)}{b}, \quad (2.3)$$

$$M' = 4\pi G \rho b^2 b' = 4\pi G \rho b^2 a E(x). \quad (2.4)$$

In Eq. (2.2) we have introduced the time-independent function

$$E(x) = b'/a \quad (2.5)$$

and Eq. (2.3) defines $M(x)$ which is also time-independent. In LTB models M/G can be interpreted as mass density (Note that in the LTB case a term $b/(2G)$ has to be added to M which is a consequence of the curvature of the 2-sphere. For more details see [17].), and $(M'/G)r^2 dr$ is the mass in a shell of thickness dr . However as the mass in an infinite plane is not well defined, this interpretation is not meaningful in the planar case. In our case it is therefore not unreasonable that M may become negative even though a , b and ρ are supposed to be positive at all times.

From the matter conservation equation we also obtain $\partial_t(\rho b^2 a) = 0$, which, on the other hand, is a consequence of Eq. (2.4).

2.1 The solutions

Eq. (2.3) can be rewritten as

$$\dot{b}^2 = \frac{2M(x)}{b} + E(x)^2, \quad (2.6)$$

with parametric solutions [12, 16]

$$\text{for } E \neq 0 : \quad b = \frac{M}{E^2} (\cosh \eta - 1) = \frac{2M}{E^2} \sinh^2(\eta/2), \quad (2.7)$$

$$t = \frac{M}{E^3} (\sinh \eta - \eta) + t_B(x), \quad \text{for } M > 0; \quad (2.8)$$

$$b = -\frac{M}{E^2} (\cosh \eta + 1) = -\frac{2M}{E^2} (\sinh^2(\eta/2) + 1), \quad (2.9)$$

$$t = -\frac{M}{E^3} (\sinh \eta + \eta) + t_B(x), \quad \text{for } M < 0; \quad (2.10)$$

$$b = |E|(t - t_B(x)) \quad \text{for } M = 0; \quad (2.11)$$

$$\text{for } E = 0 : \quad b = \left(\frac{3}{2} \sqrt{2M}(t - t_B(x)) \right)^{2/3}, \quad \text{for } M > 0, \quad (2.12)$$

$$b = b_0 = \text{const.}, \quad \text{for } M = 0. \quad (2.13)$$

Note that for $E = 0$ Eq. (2.6) implies that $M \geq 0$. This equation also implies

$$b \geq -\frac{2M}{E^2}$$

at all times, in all cases.

The function $t_B(x)$ is arbitrary; it is called the 'bang time'. For $M \geq 0$, at $t = t_B$, i.e. $\eta = 0$, we have $b = 0$ which represents the Big Bang singularity. Positions with $M < 0$ have no Big Bang singularity but a 'bounce' at $t = t_B$. We shall simplify below to the case $t_B \equiv 0$, i.e., uniform bang time. Note that we have chosen expanding solutions. From these we can obtain the collapsing solutions simply by changing the sign of t . Since in the Einstein equations only \dot{b}^2 appears they are invariant under $t \rightarrow -t$.

Of course the $\{t = \text{const.}\}$ hypersurfaces are not parallel to the $\{\eta = \text{const.}\}$ hypersurfaces, but their position depends on x . For fixed position x , Eqs. (2.7,2.8) and (2.12) correspond to Friedmann solutions with curvature $K = -E^2 \leq 0$ and $M = 4\pi G\rho b^3/3$. Note that unlike in the Friedmann case, wall solutions with $M < 0$ need not be unphysical.

The parametric representation with η is chosen in order to express the solutions in terms of elementary functions, but it is of course not necessary. For example, for $M > 0$, setting

$$\tau(t, x) = -E^2 \left(\frac{t}{6M} \right)^{2/3} \quad \text{and}$$

$$S(\tau) = (-3\tau)^{-1} \sinh^2 \left(\frac{1}{2} [\sinh - \text{id}]^{-1} (6(-\tau)^{3/2}) \right)$$

we obtain

$$b(t, x) = -\frac{M}{E^2} 6\tau S(\tau).$$

Note that in the definition of S , $[\sinh - \text{id}]^{-1}$ denotes the inverse of the function in brackets, and id is the identity function, $\text{id}(x) = x$. One can check that S solves the differential equation [18]

$$\frac{4}{3} (S + \tau S')^2 + 3\tau - \frac{1}{S} = 0, \quad (2.14)$$

with initial condition $S(0) = (\frac{3}{4})^{1/3}$. Note that this is the only regular solution, i.e. solution with $S'(0) \neq \infty$. This expression will be useful in Section 3.3.

The function $a(x, \eta)$ can be obtained from Eq. (2.5). For example for $M > 0$ we find

$$a = E^{-1} \left(\frac{\partial b}{\partial x} \right)_t$$

$$\text{for } E \neq 0 : \quad a = \frac{2}{E} \left(\frac{M}{E^2} \right)' \sinh^2 \left(\frac{\eta}{2} \right) - \coth \left(\frac{\eta}{2} \right) \left[t'_B + \left(\frac{M}{E^3} \right)' (\sinh \eta - \eta) \right], \quad (2.15)$$

$$\text{for } E = 0 : \quad a = \frac{(t - t_B)^{2/3}}{M^{1/3} 6^{1/3}} \left[M^{-1/3} \frac{M'}{E} + \frac{9(t - t_B)^{2/3} E'}{5 \times 6^{1/3}} \right]. \quad (2.16)$$

(The suffix t in $\partial b / \partial x$ indicates that we have to interpret b as functions of (t, x) , not (x, η) , in this derivative.) Even if $E = 0$, Eq. (2.4) implies that $0 < M'/E < \infty$, so that the

r.h.s. of Eq. (2.16) is well defined. Below, we shall choose the x -coordinate such that $M'/E = \text{constant}$.

Note that $M(x)$ and $E(x)$ can pass through zero so that in general different solutions from above have to be glued together at the boundary of their validity. We have checked that this gluing process can be performed in a smooth way and does not induce singularities in the scale factor b . However, for $M \rightarrow 0$ the scale factor $a \rightarrow \infty$. Nevertheless, we believe this to be a coordinate singularity, since, as we have checked, both, the Kretschmann scalar, $K \equiv R_{\alpha\beta\mu\nu}R^{\alpha\beta\mu\nu}$ and the scalar curvature remain finite for $M \rightarrow 0$. In our examples below we shall have $M > 0$ throughout and therefore we do not encounter this problem. However, when computing a from Eq. (2.5), one has to be careful to use the result (2.15) and take the limit $E \rightarrow 0$ for fixed t , hence also $\eta \rightarrow 0$. One cannot use (2.12) and (2.5), since for $E = 0$ we have $M' = 0$ so that Eq. (2.5) is identically satisfied and cannot be used to obtain $a(t, x)$.

2.2 Singularities

Singularities can occur when a , b or ρ become either infinite or zero. To have no singularities (apart from the Big Bang) which occurs at $t = t_B$, hence $b = 0$, in the past light cone of every possible observer we might be interested in, we must demand that all singularities lie in the future. In more precise models, when one specifies the observer location, one can relax this condition to the one that no singularity lies within the background lightcone of the specific observer.

In general, the question of singularities depends on the choice of the functions $M(x)$ and $E(x)$. From our solutions it is clear that b behaves monotonically as a function of time for fixed x . This is to be expected since no clustering goes on in the directions y_1 and y_2 described by this scale factor. Since we are interested in an expanding b , a singularity is present when the the scale factor a of the x -direction tends to zero. From Eq. (2.15) we infer that for $t_B \equiv 0$, $a = 0$ implies

$$\frac{2}{E} \frac{(M/E^2)'}{(M/E^3)'} = \frac{\cosh(\eta/2)}{\sinh^3(\eta/2)} (\sinh \eta - \eta) \geq 4/3.$$

It is easy to verify that the right hand side is an even positive function with minimum $4/3$ at $\eta = 0$. Hence there is a singularity at some finite value of η if the l.h.s. ever becomes larger than $4/3$ or, equivalently, if

$$\frac{E'}{E} \frac{M/E^3}{(M/E^3)'} = \frac{\cosh(\eta/2)}{2 \sinh^3(\eta/2)} (\sinh \eta - \eta) - 1 > -1/3$$

for some value of x .

We now consider a simple ansatz motivated by the perturbative analysis presented in Ref. [16]. We choose

$$M(x) = \frac{2}{9t_0^2} (1 + \epsilon h(x)) \tag{2.17}$$

and

$$4\pi G \rho b^2 a = \frac{M'}{E} = \frac{2}{3} t_0^{-2} = \text{const.} \tag{2.18}$$

so that

$$E = \epsilon \frac{h'}{3}. \quad (2.19)$$

In full generality $M'/E = f(x)$ could be an arbitrary positive function of x . But we can always make a coordinate transformation to $\tilde{x}(x)$ determined by

$$\frac{dx}{d\tilde{x}} = \frac{1}{6\pi G \rho b^2 a t_0^2},$$

so that with respect to the new coordinate $M'/E = \text{constant}$. Hence we just fix the coordinate x (up to a constant shift) by this choice. In addition, we have chosen uniform bang time, $t_B(x) \equiv 0$. This is a true restriction. With this we have reduced the three free functions of x to one, $h(x)$ which defines the density profile. Furthermore, we have introduced the parameter ϵ such that for $\epsilon = 0$ we reproduce the matter dominated Friedmann solution. We may also require $|h(x)| \leq 1$ so that ϵ indicates the amplitude of the perturbations. We do this in one of the examples below.

The above requirement for a singularity at some time $t \neq 0$ now reduces to $MM'' < M'^2/3$. (Strictly our derivation applies only for $M' \neq 0$. For $M' \propto E = 0$, one sees directly from Eq. (2.16) that $M'' \propto E' < 0$ is the necessary and sufficient condition for $a = 0$ at some time $t > t_B$.) We have found that most interesting mass profiles satisfy this condition for some values of x and therefore have singularities at some time in some places. This is not surprising but actually expected from gravitational collapse. However, when over densities become very high and we approach the collapse, pressure forces and heating become important and our simple pressure-less dust model for matter no longer holds. In order to be able to stay within the present framework, we therefore demand that such singularities be in the future and not in the past for the density profiles under consideration.

Let us consider as a first example

$$h(x) = \cos(kx).$$

Then the condition for the existence of a singularity (at $t \neq 0$) becomes

$$- (\epsilon \cos(kx) + \epsilon^2 \cos^2(kx)) < (\epsilon^2/3) \sin^2(kx),$$

which is always satisfied for some values of x , irrespective of k and ϵ . A similar behavior is expected whenever h is not a convex function, but a function representing several under- and over-densities cannot be convex.

However, this is not so important for our considerations. As we have said, the requirement of singularities to be absent is mainly a technical one and it is actually sufficient not to have a singularity in the past.

Using the above expression for a (for $M > 0$) and the ansatz (2.17,2.19) for M and E , we find that $a = 0$ is equivalent to

$$\frac{(1 + \epsilon h)h''}{\epsilon h'^2 - 3(1 + \epsilon h)h''} = -\frac{1}{3} \frac{1}{1 - \frac{\epsilon h'^2}{3(1 + \epsilon h)h''}} = \frac{1}{2} \frac{\cosh(\eta/2)}{\sinh^3(\eta/2)} (\sinh \eta - \eta) - 1 > -1/3. \quad (2.20)$$

Interestingly, in extremal positions of h , with $h' = 0$, the l.h.s. of the above expression is exactly $-1/3$. This comes from the fact that for this case $\eta = 0 \forall t$ and we have to replace the condition that there is no singularity before some given time t_0 by $a(t) > 0$ for $t < t_0$ using expression (2.16) for $a(t)$. If $h''' = 0$ when $h' = 0$ (as in our example) one can show that in the positions where h has a maximum, hence $h' = 0$ and $h'' < 0$, $1 + \epsilon h > 0$, singularities occur first. Furthermore, when $1 + \epsilon h > 0$ and $h'' < 0$, the denominator of the l.h.s. of Eq. (2.20) is larger than 1 and hence the l.h.s. becomes larger than $-1/3$. Therefore, there exists a finite value $\eta_s(x)$ where Eq. (2.20) is satisfied and $a(x, \eta_s(x)) = 0$. If, on the contrary, $1 + \epsilon h > 0$ and $h'' > 0$ the l.h.s. of Eq. (2.20) is smaller than $-1/3$. For positions in the vicinity of an extremum this implies that if the extremum is a minimum of h , the position x does not encounter a singularity in the future while positions close to maxima do.

Let us study in more detail the request that the second singularity (not the big bang one) lies in the future, $t > t_0$. Using the expression (2.8) for t , we can rewrite the condition $a(x, \eta_s) = 0$ as

$$\frac{(1 + \epsilon h)h''}{\epsilon h'^2 - 3(1 + \epsilon h)h''} = \frac{9 \cosh(\eta_s/2)}{4 \sinh^3(\eta_s/2)} \frac{t_0^2 t(x, \eta_s) \epsilon^3 h'^3}{(1 + \epsilon h)} - 1.$$

The condition $t(x, \eta_s) > t_0$, for $h' < 0$ which we shall consider hence $\eta_s < 0$ for $t(x, \eta_s) > 0$, then becomes

$$\frac{(1 + \epsilon h)}{\epsilon^3 h'^3} \left[1 + \frac{(1 + \epsilon h)h''}{\epsilon h'^2 - 3(1 + \epsilon h)h''} \right] \frac{4}{9t_0^3} < \frac{\cosh(\eta_s/2)}{\sinh^3(\eta_s/2)}.$$

This equation for $\eta_s(x)$ can only be solved numerically. However, often we realize that the l.h.s. is smallest at small $|h'|$ i.e. for small values of $|E(x)|$. Hence singularities will develop first in positions with small $|h'|$. This requires also small $|\eta_s|$ so that we may develop the scale factor a and t in η_s . The above inequality then leads to power law relations and inserting the above expression for $E = (3/2)M't_0^2$ yields the constraint

$$1 + \frac{(3t_0^2)^{7/3} 3^{1/3} 2^{2/3}}{80} \left(6M''M^{1/3} - \frac{M'^2}{M^{2/3}} \right) > 0,$$

$$1 - \frac{1}{20}(t_0 k)^{2/3} \left(6\epsilon \cos(kx) (1 + \epsilon \cos(kx))^{1/3} + \frac{\epsilon^2 (\sin(kx))^2}{(1 + \epsilon \cos(kx))^{2/3}} \right) > 0. \quad (2.21)$$

The first inequality is general while for the second inequality we have chosen $h = \cos(kx)$. In Fig. 1 we plot the constraint for this case together with the condition to use the limiting solution for $E = 0$, (2.16), (which is not necessary for our analysis) in the ϵ - λ plane, where λ denotes the wavelength of the perturbation $\lambda = 2\pi/k$.

3. The distance redshift relation in a wall universe

3.1 Generalities

3.1.1 Redshift

We now consider a photon emitted from a source at some position and time (t_s, \mathbf{x}_s) arriving in our telescope at position and time (t_0, \mathbf{x}_0) . We denote the matter 4-velocity field, hence

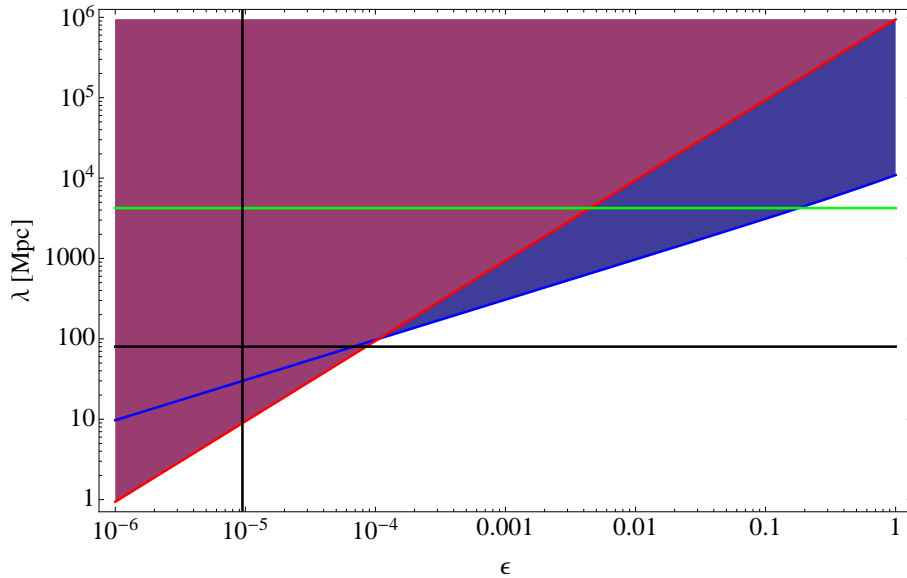


Figure 1: The region above the red line has singularities in the future only. While the blue line describes the condition to use the limiting solution for $E = 0$, (2.16). This can be used when $tE^3/M \ll 1$, where with " \ll " we mean at least two orders of magnitude smaller. The two black lines describe the physical parameters $\epsilon = 9.5 \times 10^{-6}$ and $\lambda = 80$ Mpc. The green line is the Hubble scale H_0^{-1} . With physical parameters we mean an amplitude as determined by WMAP [19] observations and a wavelength agrees with the size of the largest observed voids [20] which is about 40-90 Mpc. More precisely we find ϵ requiring that at early time there is only a single density fluctuation in each Hubble distance. This leads, at first order, to $\delta = 8\pi^2\epsilon/15$, and the matter density fluctuation at early times, $\delta \cong 5 \times 10^{-5}$ can be inferred from WMAP observations. For more details see [15].

the 4-velocity of source and observer by $u(t, \mathbf{x})$ and the photon 4-velocity by n . The redshift of the source, z is then given by

$$1 + z = \frac{g(n, u)|_s}{g(n, u)|_0}. \quad (3.1)$$

We consider a co-moving source and observer, hence $u = \partial_t$ and normalize the affine parameter of the photon, s , such that $n^0(s_0) = 1$. The redshift then reduces to

$$1 + z = n^0|_s \quad (3.2)$$

for our geometry with $g_{00} = -1$ and $g_{0i} = 0$. From the geodesic equation for the photon we infer that its momenta in y_1 - and y_2 -direction are simply redshifted so that

$$J_1 \equiv b^2 n^1 = b^2 \frac{dy_1}{ds} = \text{const.} \quad \text{and} \quad J_2 \equiv b^2 n^2 = b^2 \frac{dy_2}{ds} = \text{const.} \quad (3.3)$$

hence

$$(n^x)^2 = \left(\frac{n^0}{a}\right)^2 - \frac{1}{a^2 b^2} (J_1^2 + J_2^2). \quad (3.4)$$

From the geodesic equation for n^0 we can now derive the evolution of the redshift:

$$\frac{dz}{ds} = -\frac{dn^0}{ds} = (1+z)^2 \frac{\dot{b}'}{b'} + \frac{J_1^2 + J_2^2}{b^2} \left(\frac{\dot{b}}{b} - \frac{\dot{b}'}{b'} \right). \quad (3.5)$$

Here we have used $a = b'/E$ to eliminate the scale factor a . Note also that the prime and the dot in the above equation denote partial derivatives while d/ds is a total derivative along the path of the photon.

3.1.2 Distance

The evolution of the distance to the source is given by the Sachs focussing equation [21],

$$\frac{d^2 D}{ds^2} = -(|\sigma|^2 + \mathcal{R}) D. \quad (3.6)$$

D is the angular diameter distance to the source, σ is the complex scalar shear of the light bundle which we define below and

$$\mathcal{R} = \frac{1}{2} R_{\mu\nu} n^\mu n^\nu = 4\pi G T_{\mu\nu} n^\mu n^\nu = 4\pi G (1+z)^2 (\rho + \bar{P}). \quad (3.7)$$

Here \bar{P} is the pressure in the direction of the photon. The important point is that this quantity is non-negative for any energy momentum tensor which satisfies the dominant energy condition $\rho \geq \bar{P}$ in all directions, hence also for a cosmological constant where we have $\mathcal{R} \equiv 0$. In terms of the affine parameter of the photon, the growth of the angular diameter distance to the source is not accelerated. If the dominant energy condition is satisfied $D(s)$ is always a concave function. Furthermore, clustering which leads to the production of non-vanishing shear is only increasing the deceleration of D as function of the affine parameter s . But of course we do not measure this function but $D(z)$ which can behave very differently.

The complex shear of the light ray bundle is defined as follows (appendix 7.7.3. in [22]): We consider two spatial orthonormal vectors e_1 and e_2 which are normal to both, u and n at the observer and are parallel transported along n , such that $\nabla_n e_a = 0$ for $a = 1, 2$. The vectors e_1, e_2 are a basis of the so called 'screen'. Note that we do not require that u be parallel transported along n , hence e_1, e_2 are in general not normal to u elsewhere than at the observer, where we have given their initial conditions. The complex shear is defined by

$$\sigma = \frac{1}{2} g(\epsilon, \nabla_\epsilon n), \quad \epsilon \equiv e_1 + i e_2. \quad (3.8)$$

In order to compute the shear we must know n not only along the photon geodesic itself but we must determine its derivatives in directions normal to n . We shall directly use the transport equations [22]. For a vorticity free ray bundle (which is the case here) with expansion rate $\theta \equiv \frac{1}{2} n^\mu_{;\mu}$ these are

$$\dot{\theta} + \theta^2 + \sigma_1^2 + \sigma_2^2 = -\mathcal{R}, \quad (3.9)$$

$$\dot{\sigma}_1 + 2\theta\sigma_1 = -\text{Re}(\mathcal{F}), \quad (3.10)$$

$$\dot{\sigma}_2 + 2\theta\sigma_2 = \text{Im}(\mathcal{F}), \quad (3.11)$$

where $\sigma_1 = \text{Re}(\sigma)$, $\sigma_2 = \text{Im}(\sigma)$, and $\mathcal{F} = \frac{1}{2}R_{\alpha\mu\beta\nu}\bar{\epsilon}^\alpha\bar{\epsilon}^\beta n^\mu n^\nu$. To determine the shear σ we need to know the initial conditions for the differential equations (3.9) to (3.11). It is possible to determine the behavior of the shear and the expansion of the light near the vertex [23]. Choosing the affine parameter of the photon to vanish at the observer position, $s_0 = 0$, these are

$$\sigma(s) = -\frac{s}{3}\bar{\mathcal{F}}_0 + O(s^2), \quad (3.12)$$

$$\theta(s) = \frac{1}{s}\left(1 - \frac{1}{3}\mathcal{R}_0 s^2\right) + O(s^3). \quad (3.13)$$

\mathcal{F}_0 and \mathcal{R}_0 are the values of \mathcal{F} and \mathcal{R} at the observer position. The light bundle expansion θ diverges at the observer position, but we can consider an initial condition not exactly at the observer. This choice can affect the numerical precision. After determining \mathcal{R} , ϵ and \mathcal{F} for a given geometry and photon direction, we can solve the system (3.9) to (3.11) together with the Sachs focusing equation (3.6) numerically.

3.2 'Realistic' walls

We want to investigate whether the system of equations derived above for $z(s)$ and $D(s)$ can lead to a distance-redshift relation close to the one observed. For wall universes we consider,

$$\mathcal{R} = 4\pi G\rho(1+z)^2 = \frac{2(1+z)^2}{3t_0^2 b^2 a}. \quad (3.14)$$

For a chosen density contrast $h(x)$ we can determine $b(t, x)$ and $a(t, x)$ and solve the photon geodesic Eq. (3.5) for a given angle θ_0 of the observed photon w.r.t. the y -plane,

$$\cos\theta_0 = \frac{\sqrt{J_1^2 + J_2^2}}{b(x_0, t_0)n^0(0)}. \quad (3.15)$$

We again set the initial value or the affine parameter to 0, hence $x_0 = x(0)$ etc.

We have investigated two choices for $M(x)$. The first is simply $M(x) = \frac{2}{9t_0^2}(1 + \epsilon \cos(kx))$ which we have already discussed before. The results for this case are shown in Fig. 2.

The result is quite striking: The deviation from the Einstein-de Sitter distance-redshift relation is very small. On the level of a few percent in the most extreme case. Much smaller than the deviation for an open (Milne) Universe or even for Λ CDM. Hence voids and walls with the chosen parameters cannot simulate the observed distance redshift relation. We have also studied different values of the parameters (ϵ, k) , but all cases which are such that there is no singularity before t_0 lead to small deviation from Einstein-de Sitter. Only for wavelengths of approximately Hubble scale, $k \sim H_0$, where we can choose $\epsilon \sim 10^{-3}$ do the deviations become relatively large. But the density profile chosen here does not at all lead to a relation that resembles the observations.

As a second profile we consider thin, highly concentrated over-dense walls with an exponential profile:

$$h(x) = \frac{\lambda}{\sqrt{2\pi\sigma^2}} \sum_i \exp\left(\frac{-(x-x_i)^2}{2\sigma^2}\right) - 1, \quad (3.16)$$

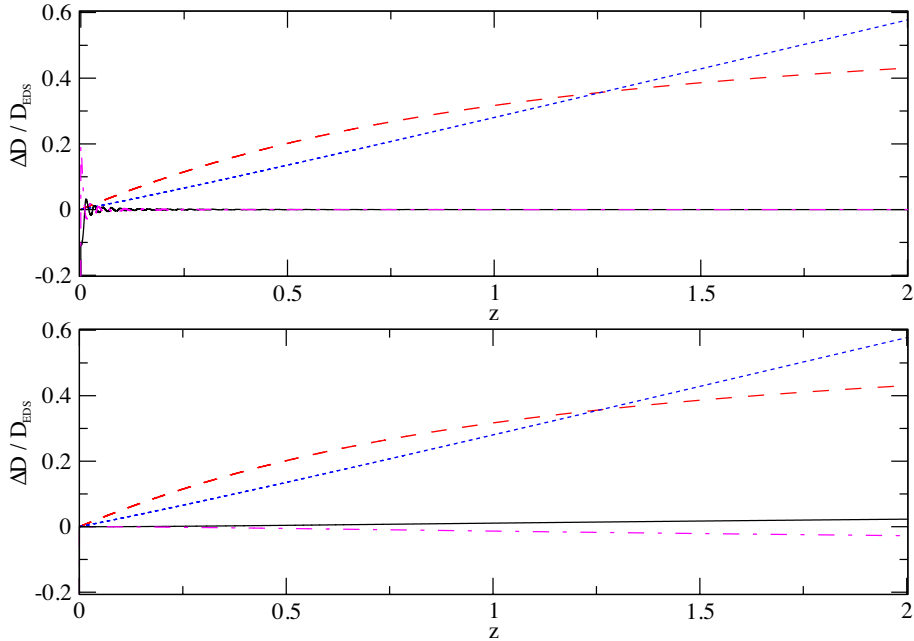


Figure 2: We show the relative luminosity distance redshift relation $\frac{\Delta D(z)}{D_{EdS}(z)} = \frac{D(z) - D_{EdS}(z)}{D_{EdS}(z)}$, for different models with luminosity distance $D(z)$. The blue dotted curve is for a Milne Universe, the red dashed curve is for Λ CDM universe with $\Omega_\Lambda = 0.7$ and $\Omega_M = 0.3$. The remaining two lines are our wall universe. The black solid line is in an under density while the purple dot-dashed line is in an over density. In the top panel, we consider light propagating in the x -direction only. The bottom panel is the same but for light propagating in the y -direction. The parameters for the wall model are the physical ones, $\epsilon = 9.5 \times 10^{-6}$ and $\lambda = 80$ Mpc.

where $\lambda = x_{i+1} - x_i$. In the limit $\sigma \ll \lambda$ the mean of $h(x)$ vanishes and $\min_x h(x) = -1$. Again, we choose ϵ such that there is no singularity before t_0 . The results for this profile are shown in Fig. 3.

We have obtained the following result in these two examples (and other profiles which we do not present here explicitly): The modification of $D(z)$ never goes beyond the case of the open universe. We do not obtain acceleration by a series of dense walls. Even though we present here only two simple profiles, we think the conclusion is valid beyond these cases: if a photon passes through many *compensated* under- and over-densities in the integrated distance $D(z)$ the effect is minute as long as the time the photon spends inside a wall is much smaller than the time scale at which the gravitational potential of the wall evolves. A perturbative (first order) calculation gives a flavour of this effect. Indeed, at first order in the perturbed direction, the difference between $D(z)$ in our models and $D_{EdS}(z)$ of a matter dominated universe can be written as

$$\begin{aligned}
 D_L(z_e) - D_L^{EdS} &= (1 + z_e) (\eta_o - \eta_e) \left(\frac{\epsilon}{3} (h(\eta_o) + h(\eta_e)) \right) - (1 + z_e) \int_{\eta_e}^{\eta_o} \frac{2\epsilon}{3} h(\eta) d\eta \\
 &+ (1 + z_e) \int_{\eta_e}^{\eta_o} d\eta \int_{\eta_e}^{\eta} d\eta' \frac{\epsilon}{15} h''(\eta') \eta' - \frac{1 + z_e}{\mathcal{H}_e} \int_{\eta_e}^{\eta_o} d\eta \frac{\epsilon}{15} h''(\eta) \eta, \quad (3.17)
 \end{aligned}$$

where the subscripts e and o respectively mean that the conformal time is evaluated at the

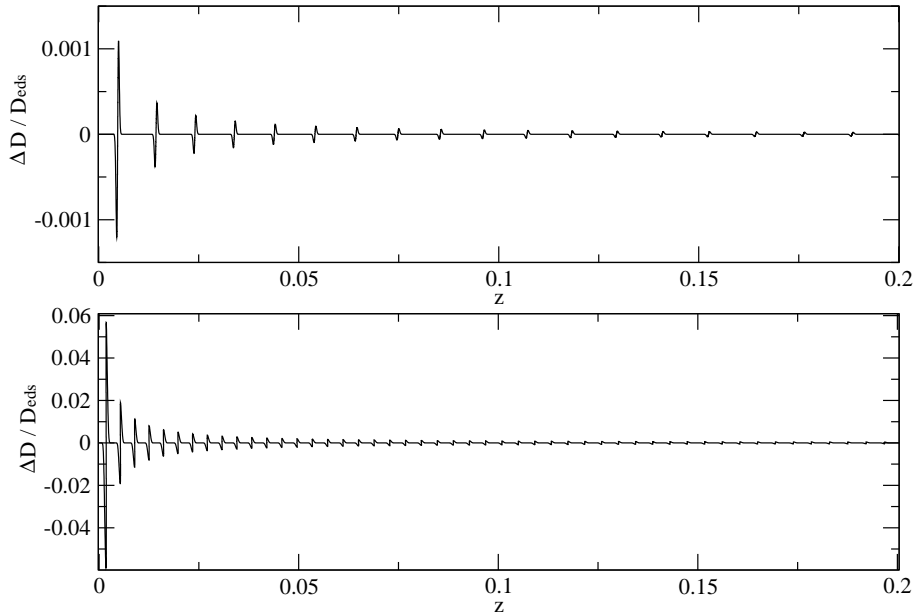


Figure 3: We show the relative difference between the distances in 'realistic' wall models and in EdS universe for photons propagating in x -direction. The top panel is obtained with $\epsilon = 10^{-9}$, $\lambda = 40$ Mpc and $\sigma = 1$ Mpc, while the bottom one with $\epsilon = 5 \times 10^{-8}$, $\lambda = 15$ Mpc and $\sigma = 1$ Mpc. In both cases the observer is at the center of the void. We have checked that the order of magnitude does not change for an observer in an over density. In the second case, we see that we obtain an effect of the same order of magnitude as the swiss cheese universe discussed in [24].

source (emission) or at the observer and expresses the perturbation of the energy density in under and over densities (see Appendix C for a derivation of the linearized result). From this expression, valid in the linear regime only, and for a periodic perturbation, it becomes clear that the deviation of $D_L(z)$ with respect to D_L^{EdS} depends on the amplitude ϵ of the perturbation and on the values of the conformal time at the source and at the observer. In the case of periodic perturbations, the contributions from photon path are mostly cancelled in the integral terms. Of course in the full non-linear calculation there is no simple relation between the matter over density h and the gravitational potential. In this case in principle the full non-linear Einstein equation have to be solved and Eqs. (3.5) and (3.6) govern $D_L(z)$.

Surprisingly, however, our non-linear simulations show that this result holds also to some extent in the non-linear regime. Note that, even though our value of ϵ is small, the over densities in the walls are large at late times, such that they develop singularities soon after today and we are deeply in the non-linear regime. While we do not have a proof that our conclusion holds in all cases, we have tested this also with other periodic wall profiles.

In Fig. 4 we show the deviations of the expansion rates with respect to the Hubble expansion in EdS universe. We note that the deviations in the unperturbed directions are small. However, in the perturbed direction these deviations can be large locally inside a wall, and they would be measurable by direct, local measurements of $H(z)$. However, they compensate when averaged over a wall thickness and do not show up in integrated

quantities like $D(z)$.

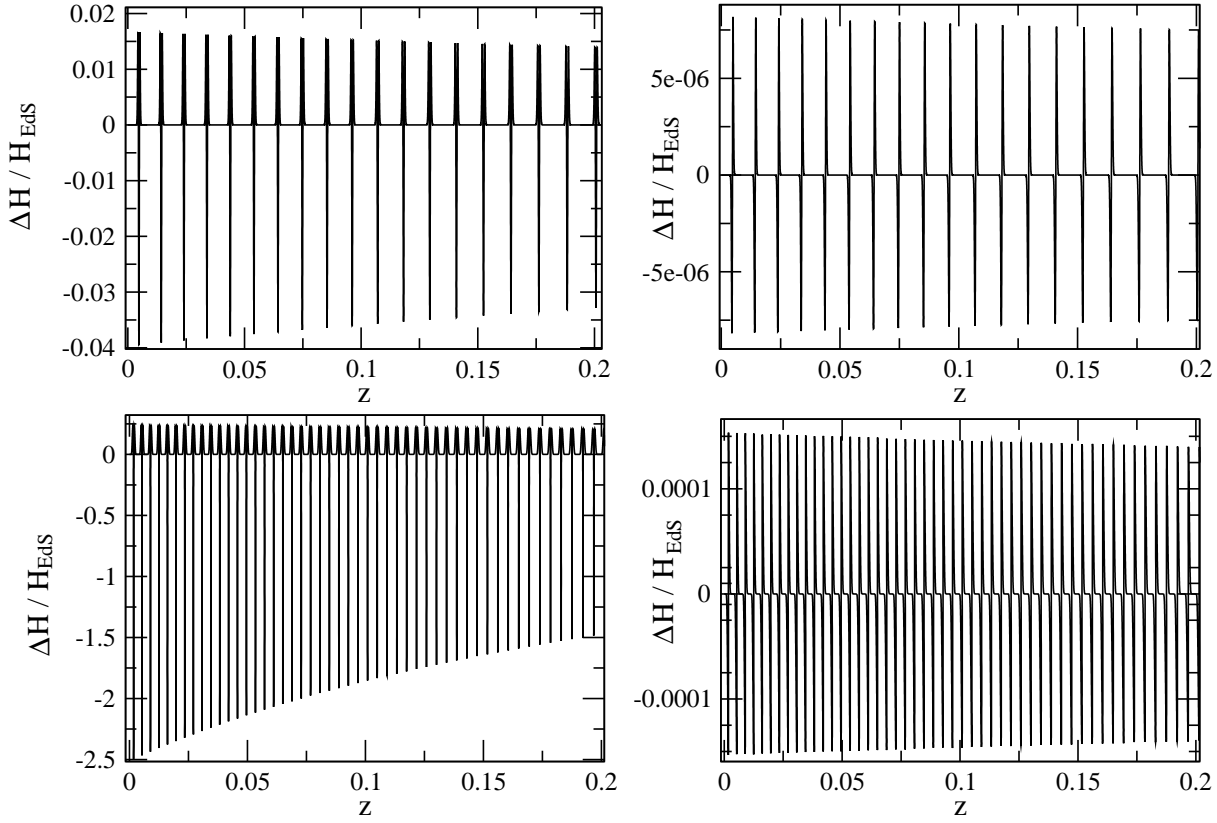


Figure 4: We show the relative differences between the expansion rates in the thin, highly concentrated over-dense wall model and the Hubble expansion in EdS universe. The top panels are obtained with $\epsilon = 10^{-9}$, $\lambda = 40$ Mpc and $\sigma = 1$ Mpc, while the bottom ones with $\epsilon = 5 \times 10^{-8}$, $\lambda = 15$ Mpc and $\sigma = 1$ Mpc. In both cases the observer is at the center of the void. The left panels show the expansion rates in the perturbed direction, while the right ones in the y-direction. The results for the cosine profile not shown here are similar to the two top panels.

3.3 Mimicking dark energy

Yoo et al. [18] have shown that in an LTB model every given distance–redshift relation can be mimicked by a suitable choice of the density profile. The same is true for a wall universe. For a given function $D(z)$ we can find a density profile which leads to exactly this distance–redshift relation for a photon coming in x -direction. First of all, for such a photon the shear vanishes for symmetry reasons and \mathcal{R} is given by (3.14). To find the density profile, which is equivalent to finding $M(x)$ or $M(z) \equiv M(x(z))$ we have to solve the following coupled system of six ordinary differential equations (in principle none of the other equations couples to (3.20) since both, F_M and F_β do not depend on x explicitly),

which is very similar to the system solved in Ref. [18]:

$$\frac{dM}{ds} = F_M(t, z, M, \beta, \zeta), \quad (3.18)$$

$$\frac{d\beta}{ds} = F_\beta(t, z, M, \beta, \zeta), \quad (3.19)$$

$$\frac{dx}{ds} = \frac{F_M(t, z, M, \beta, \zeta)}{\beta}, \quad (3.20)$$

$$\frac{dt}{ds} = 1 + z, \quad (3.21)$$

$$\frac{dz}{ds} = \frac{\zeta}{\frac{dD}{dz}}, \quad (3.22)$$

$$\frac{d\zeta}{ds} = -4\pi(1+z)^2 \rho D, \quad (3.23)$$

where we have defined

$$\zeta = \frac{dz}{ds} \frac{dD}{dz} \quad \text{and} \quad \beta = \frac{dM}{\frac{dx}{ds}} = M' = \frac{2}{3t_0^2} E. \quad (3.24)$$

In Appendix A we give the derivation of this system and the detailed expressions for F_M and F_β . There, we also explain the method used to specify the initial conditions at the observer. All the constraints are fixed by requiring the system to have no critical points. Note also that $z(s)$ need not to be monotonic. If $dz/ds = 0$ at a value of s where $\zeta = dD/ds \neq 0$, the derivative dD/dz is not well defined. This is, however, not the case of a Λ CDM Universe which we want to mimic here. We are then left with one initial condition, which we choose by requiring

$$H_0 = \left. \frac{\dot{a}}{a} \right|_{s_0} = \left. \frac{\dot{b}}{b} \right|_{s_0}, \quad (3.25)$$

i.e. the value of the Hubble rate at the observer today does not depend on direction. In Fig. 5 we show $M(x)$ as well as its derivative with respect to the x coordinate, $\beta(x)$, for the solution mimicking the Λ CDM expression for $D(z)$, for $\Omega_K = 0$, $\Omega_m = 0.3$ and $\Omega_{DE}(z) = 0.7 = \text{constant}$.

$$D(z) = \frac{1}{1+z} \chi_K \left(\int_0^z \frac{dz'}{H(z')} \right) \quad \text{where} \quad (3.26)$$

$$\chi_K(r) = \frac{1}{\sqrt{K}} \sin(r\sqrt{K}), \quad \text{and}$$

$$H(z) = H_0 \left(\Omega_m(1+z)^3 + \Omega_K(1+z)^2 + \Omega_r(1+z)^4 + \Omega_{DE}(z) \right)^{1/2}.$$

In Fig. 6, we show how the luminosity distance deviates when the observer looks at photons coming in with different angles θ_0 . For $\theta_0 = 90$ degrees, we have photons traveling in x -direction, in this case the luminosity distance is fitted to the one of Λ CDM by solving the system of Eqs. (3.18-3.23) with the functions $M(x)$ and $\beta(x)$ shown in Fig. 5. It is

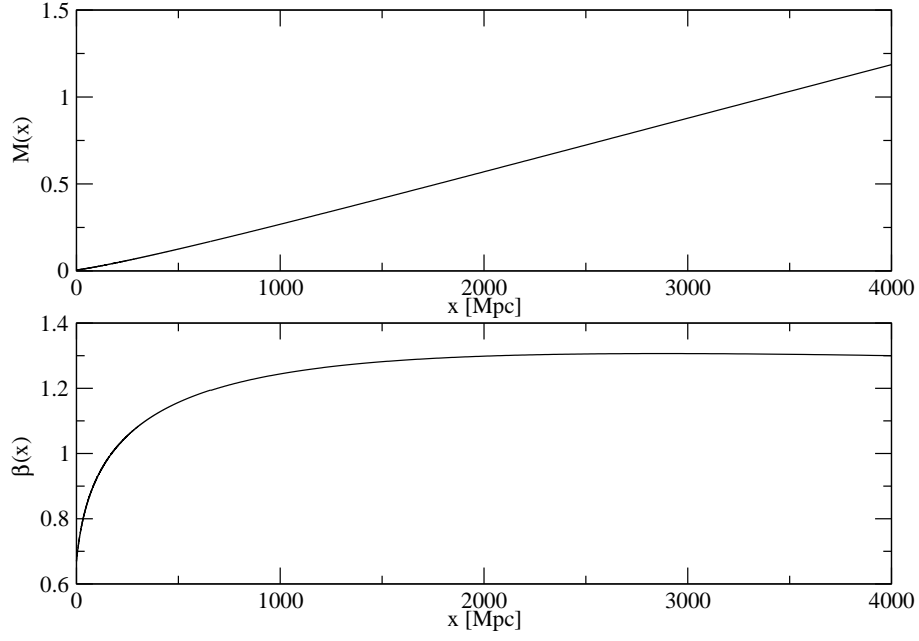


Figure 5: We show the function $M(x)$, top panel, and its derivative $\beta(x)$, bottom panel. In principle, there is a entire family of functions $M(x)$ parametrized by the initial value $M(0) = M_0$ that we are free to choose (appendix A). Here, we present the solutions corresponding to $H_0 = \left. \frac{\dot{a}}{a} \right|_{s_0} = \left. \frac{\dot{b}}{b} \right|_{s_0}$.

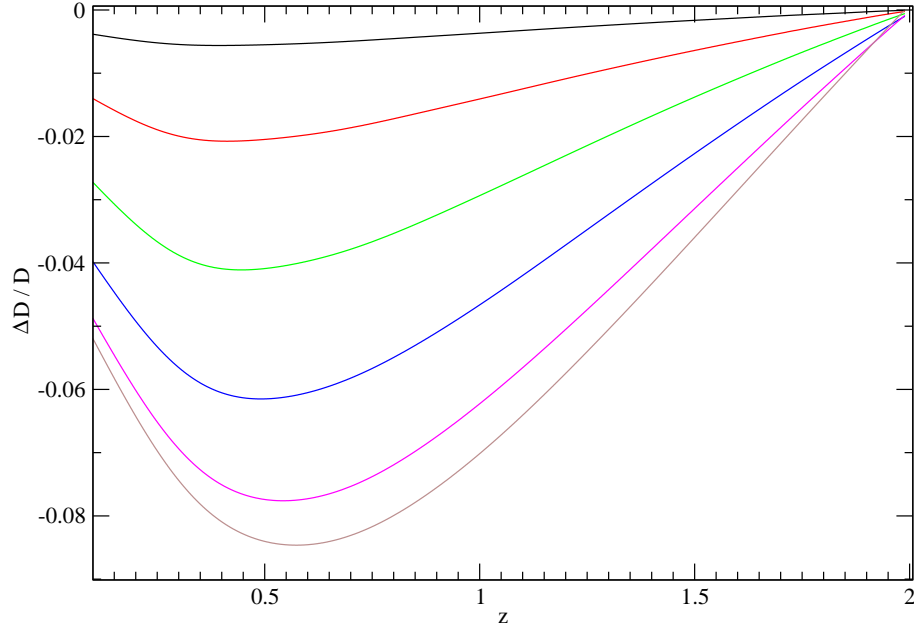


Figure 6: We show the relative differences between luminosity distances for photons traveling in the x -direction (perpendicular to the walls) and photons observed with an angle θ_0 (see Eq.(3.15)). From the top to the bottom, we respectively have $\theta_0 = 75, 60, 45, 30, 15, 5$ degrees.

interesting to remark that a given angle of $\theta_0 \in [0; 90]$ degrees at the observer corresponds to an angle at the emission $\theta_e > \theta_0$. This is a consequence of the spacetime geometry induced by the walls: due to the clustering in direction x , corresponding to $\theta = 90^\circ$, its expansion slows down in time.

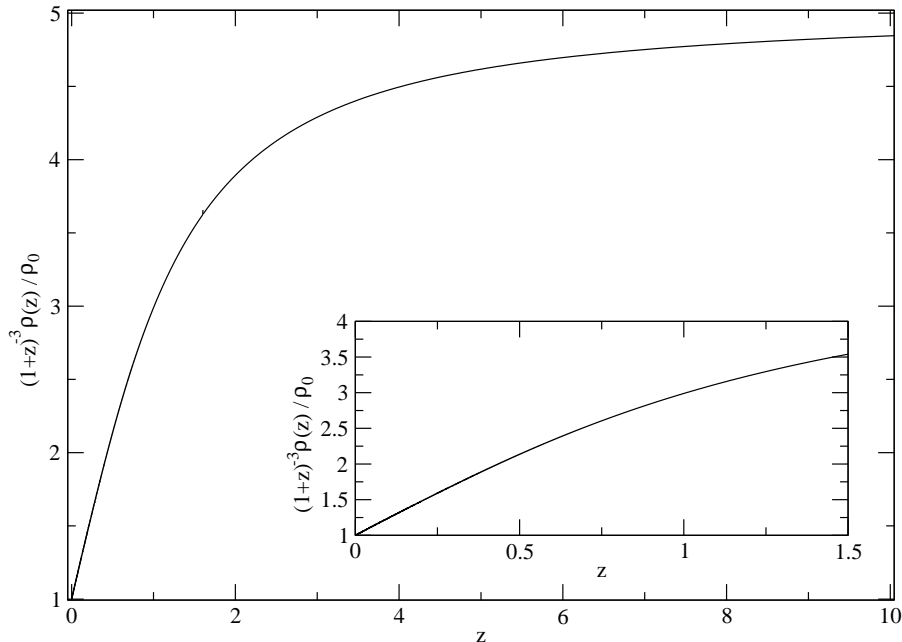


Figure 7: We show the ratio of our density profile to the Einstein-de Sitter one as a function of the cosmological redshift.

In Fig. 7, we present the density profile corrected by the isotropic expansion rate, $(1+z)^{-3}\rho(z)/\rho_0$, $\rho_0 = \rho(z=0)$, obtained for our model to mimic Λ CDM luminosity distance. Finally, in Fig. 8, we plot the expansion rates in the longitudinal and transverse directions, $H_a = \dot{a}/a$ and $H_b = \dot{b}/b$. It is interesting to estimate roughly the features of the under density needed to fit Λ CDM luminosity distance. For example, if one considers the highest redshift for which we have data from supernovae, at around $z \sim 1.7$. This roughly corresponds to a size $\sim H_0^{-1}$. (Of course we have another data point from the CMB. The angular size of the acoustic oscillations provides an excellent measure of the angular diameter distance to the last scattering surface, $z \simeq 1090$. But this is not very relevant in our context as the Universe is to a good approximation matter dominated from $z = 2$ to $z = 1090$.) An under density of the size of the order of the Hubble distance is necessary to mimic Λ CDM with our walls. Moreover, we can also determine the ratio of the energy density normalized at the observer to the energy density in an Einstein-de Sitter model at $z \sim 1.7$ which is about 4. At high redshift, $z \gtrsim 10$ the anisotropy is very small and the Universe is close to a Friedmann Universe with about 5 times the matter density obtained from local estimates.

3.4 Redshift drift

In the previous section we have fixed $M(x)$ to reproduce the distance redshift relation of

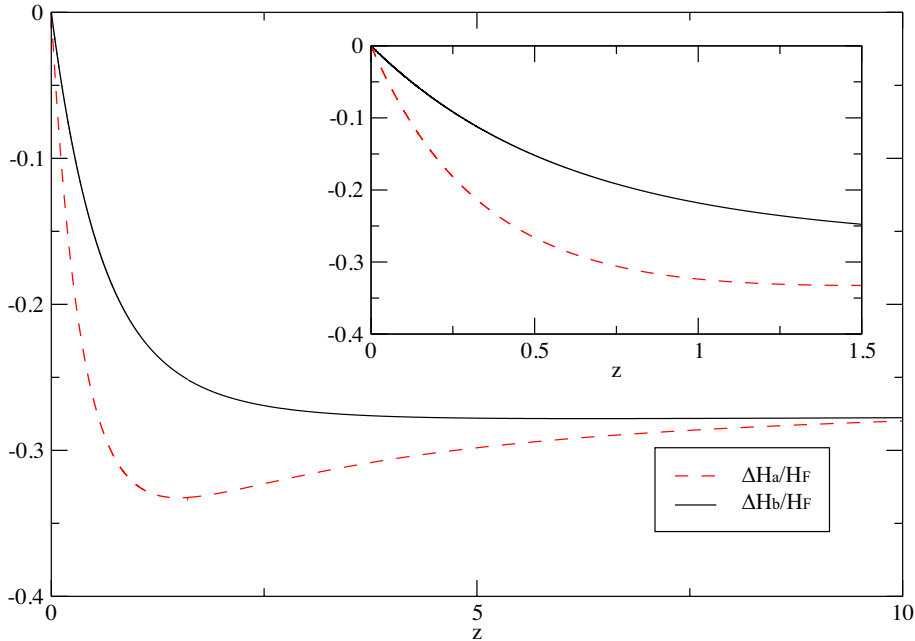


Figure 8: We show the relative expansion rates in the transverse and longitudinal directions as functions of the cosmological redshift. We use the following notation : $\Delta H_{a,b} = H_{a,b} - H_F$, where H_F is the expansion rate in an Einstein-de Sitter universe, and $H_{a,b}$ are the expansion rates in the longitudinal and transverse directions, normalized to the their values at the observer.

Λ CDM universe. Of course, having one free function to play with, namely $M(x)$, we expect to be able to fit one function, in our case $D(z)$. If we now proceed to another, independent observable, we shall most probably not fit it. We have done this by looking at the redshift drift, defined as the rate of change of the redshift of a co-moving source per unit of observer time. In a Friedmann Universe the redshift drift is simply

$$\frac{dz}{dt_0} \equiv \lim_{\Delta t_0 \rightarrow 0} \frac{z(t_s + \Delta t_s) - z(t_s)}{\Delta t_0} = H_0(1+z) - H(z), \quad (3.27)$$

where $H(z) = H(t_s)$ and H_0 denote the Hubble parameter at the source position at time t_s and at the observer at the moment t_0 . We have computed the corresponding function (for light rays in x -direction) from our solution $M(x)$. The general expression for the redshift drift of a wall Universe in x -direction is (see Appendix B),

$$\begin{aligned} \frac{dz}{dt_0} &= (1+z) \int_0^z \left(\frac{\ddot{b}'}{\dot{b}'} \right) (1+z')^{-2} dz' \\ &= -(1+z) \int_0^z \left(4\pi G\rho - \frac{2M}{b^3} \right) \frac{a}{\dot{a}} (1+z')^{-2} dz'. \end{aligned} \quad (3.28)$$

Since we do not require $M_0 = 0$ as in LTB model, we can in principle have a positive redshift drift at low redshift; but we do not obtain this for our best fit profile $M(x)$ with $t_B(x) \equiv 0$. The result is compared with Λ CDM in Fig. 9.

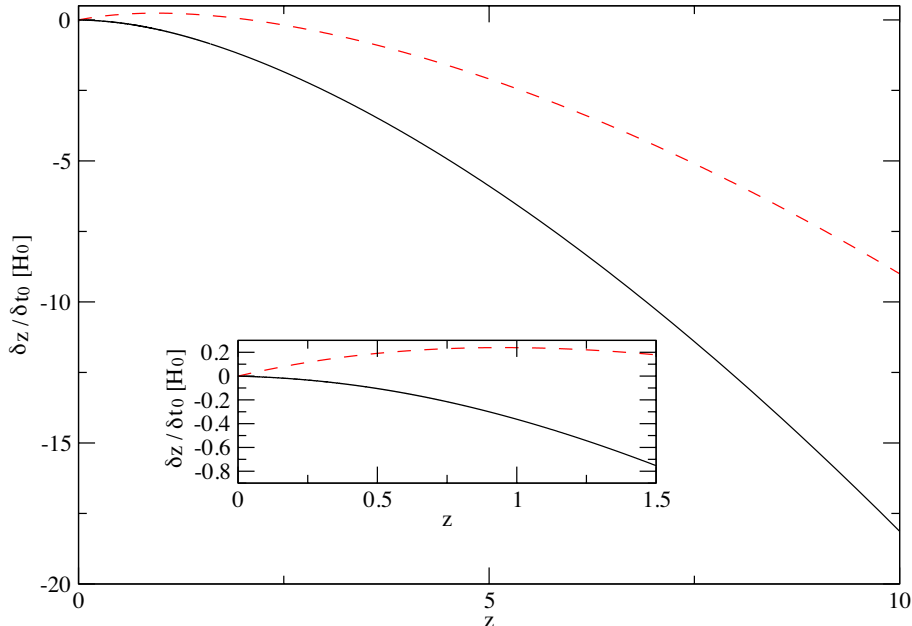


Figure 9: We show the redshift drift for the wall Universe (black solid line) which mimics the distance redshift relation of Λ CDM and compare it with the redshift drift of the latter (red dashed line).

Clearly the redshift drift for the two cosmologies are very different. We do have a second function to play with, the bang time $t_B(x)$, so that we could probably fix this observable. This has been done for LTB models in [25]. However, as it is shown there, models which have both, the same redshift distance relation and the same redshift drift as Λ CDM can be ruled out with a third observable, the kinematic Sunyaev-Zel'dovich effect which comes from the recession velocity of clusters.

4. Conclusions

We have studied the effect of matter perturbations on the luminosity distance in a model with planar symmetry described by the metric (2.1). Considering 'realistic' walls we find that the effect from density inhomogeneities is very small, it nearly averages out. It leads to fluctuations of the luminosity distance around the 'background' distance, but not to a significant global shift. Our results (Fig. 3) show that these fluctuations are due to matter inhomogeneities at the source and the observer positions, without any relevant contribution from the integrated effects of light propagation, like in the linear approach (3.17). Hence we can not mimic acceleration with many dense walls which grow by gravitational instability. Since we consider pressure-less matter only, the amplitude of density fluctuations is limited by the presence of singularities. This is a limitation of the model.

After having shown that 'realistic' wall models can not reproduce the observed distance-

redshift relation, we have determined the density profile which can mimic it. We have fixed the free function of our model, $M(x)$, to mimic the luminosity (or angular) distance of the Λ CDM universe. We have shown that the observation of the redshift drift can distinguish between this model and Λ CDM. Abandoning the assumption of an uniform bang time we could arrange the second degree of freedom, $t_B(x)$, to fit the redshift drift too. We have found that the redshift drift in our model can be positive at low redshift, contrarily to the LTB model [26].

With our solution $M(x)$ we can fit Λ CDM distance for photons coming in x -direction for positive x only. This preferred direction corresponds to the radial incoming direction for LTB model. The deviation from Λ CDM for photons coming from different angles is typically a few percent (see Fig. 6).

Acknowledgements

This work is supported by the Swiss National Science Foundation.

A. Derivation of the system of differential equations and initial conditions

A.1 The system

Here we derive in more detail the system (3.18) to (3.23) and give the initial conditions used for the solution.

Since we choose the photon affine parameter such that $n^0|_0 = 1$ we have

$$1 + z(s) = n^0(s) = \frac{dt}{ds}.$$

Furthermore, the null condition for a light ray in x -direction implies

$$\left(\frac{dt}{ds}\right)^2 = \left(\frac{b'}{E}\right)^2 \left(\frac{dx}{ds}\right)^2 = \left(\frac{2b'}{3t_0^2 M'}\right)^2 \left(\frac{dx}{ds}\right)^2. \quad (\text{A.1})$$

The geodesic equation gives

$$\frac{dz}{ds} = \frac{d^2 t}{ds^2} = -\frac{\dot{a}}{a}(1+z)^2 = -\frac{\dot{b}'}{b'}(1+z)^2. \quad (\text{A.2})$$

Hence, when the expansion in x -direction changes into contraction, $\dot{a} = 0$, also dz/ds passes through zero. However, this does not happen in our case which mimics Λ CDM. Noting that geodesics in x -direction have no shear, the Sachs focusing equation yields

$$\frac{d^2 z}{ds^2} \frac{dD}{dz} + \left(\frac{dz}{ds}\right)^2 \frac{d^2 D}{dz^2} = -4\pi G \rho (1+z)^2 D, \quad (\text{A.3})$$

where we have used $\mathcal{R} = 4\pi G (1+z)^2 \rho$. We can now rewrite these equations in terms of the system (3.18) to (3.23). To find the functions F_M and F_β we first derive the following

useful relations

$$\dot{\tau} = \frac{2}{3t}\tau, \quad (\text{A.4})$$

$$\tau' = \tau \left(2 \frac{\frac{d\beta}{ds}}{\frac{dM}{ds}} - \frac{2}{3} \frac{\beta}{M} \right), \quad (\text{A.5})$$

$$b' = -\frac{8}{9t_0^4} \frac{\tau}{\beta} (S - 2\tau S') - \frac{16}{3t_0^4} \tau^2 \frac{M}{\beta^2} \frac{\frac{d\beta}{ds}}{\frac{dM}{ds}} S', \quad (\text{A.6})$$

$$\dot{b}' = -\frac{16}{27t_0^4} \frac{\tau}{t} \frac{1}{\beta} (S - 3\tau S' - 2\tau^2 S'') - \frac{32}{9t_0^4} \frac{M}{\beta^2} \frac{\frac{d\beta}{ds}}{\frac{dM}{ds}} \frac{\tau^2}{t} (2S' + \tau S''). \quad (\text{A.7})$$

Here S' always indicates the derivative of S with respect to its argument τ while as for all other functions of (t, x) the prime denotes the partial derivative w.r.t. x and the dot the one w.r.t. t . The null condition for the light ray can be written as

$$\frac{dM}{ds} A_1 + \frac{d\beta}{ds} B_1 = \pm 1,$$

with

$$A_1 = -\frac{16}{27t_0^6} \frac{\tau}{\beta^3 (1+z)} (S - 2\tau S'), \quad (\text{A.8})$$

$$B_1 = -\frac{32}{9t_0^6} \frac{\tau^2 M}{\beta^4 (1+z)} S'. \quad (\text{A.9})$$

The geodesic equation takes the form

$$\frac{dM}{ds} A_2 + \frac{d\beta}{ds} B_2 = 0, \quad (\text{A.10})$$

where

$$A_2 = -\frac{\zeta}{\frac{dD}{dz}} \frac{8}{9t_0^4} \frac{\tau}{\beta} (S - 2\tau S') - (1+z)^2 \frac{16}{27t_0^4} \frac{\tau}{t} \frac{1}{\beta} (S - 3\tau S' - 2\tau^2 S''), \quad (\text{A.11})$$

$$B_2 = -\frac{\zeta}{\frac{dD}{dz}} \frac{16}{3t_0^4} \tau^2 \frac{M}{\beta^2} S' - (1+z)^2 \frac{32}{9t_0^4} \frac{M}{\beta^2} \frac{\tau^2}{t} (2S' + \tau S''), \quad (\text{A.12})$$

with $\zeta = \frac{dD}{ds} = \frac{dz}{ds} \frac{dD}{dz}$. From this we infer

$$F_M(t, z, M, \beta, \zeta) = \pm \frac{B_2}{A_1 B_2 - A_2 B_1}, \quad (\text{A.13})$$

$$F_\beta(t, z, M, \beta, \zeta) = \mp \frac{A_2}{A_1 B_2 - A_2 B_1}. \quad (\text{A.14})$$

Since τ is a function of M , β and t , we now have expressed everything in terms of our variables (t, z, M, β, ζ) and the given function $D(z)$. Explicitly, F_M and F_β are given by

$$F_M = \pm \frac{3t_0^2}{4} \beta \left(\frac{6M}{t} \right)^{2/3} \frac{\frac{\zeta}{\frac{dD}{dz}} \frac{3t}{2} \frac{S'}{1+z} + (1+z) (2S' + \tau S'')}{SS' + \tau SS'' - \tau S'^2}, \quad (\text{A.15})$$

$$F_\beta = \pm \frac{1}{18t_0^2} \frac{1}{M} \left(\frac{6M}{t} \right)^{4/3} \frac{\frac{\zeta}{\frac{dD}{dz}} \frac{3t}{2} \frac{(S-2\tau S')}{1+z} + (1+z) (S - \tau S' - 2\tau^2 S'')}{SS' + \tau SS'' - \tau S'^2}. \quad (\text{A.16})$$

A.2 Initial conditions

Let us now turn to the initial conditions at $s_0 = 0$. Without loss of generality we can set $x(0) = 0$. Clearly also $z(0) = 0$. From definition (3.24) we have

$$\zeta(0) = \left. \frac{dD}{ds} \right|_{s=0}. \quad (\text{A.17})$$

Since this is an initial condition for the Sachs focusing equation, we have consistently with our affine parameter normalization [23, 27],

$$\zeta(0) = -1. \quad (\text{A.18})$$

From (3.22) we note that our system of coupled differential equations has a critical point z_{cr} defined by

$$\left. \frac{dD}{dz} \right|_{z=z_{cr}} = 0. \quad (\text{A.19})$$

For our Λ CDM parameters $z_{cr} \approx 1.6$. To obtain a regular solution we must therefore impose $\zeta(z_{cr}) = 0$. We remark that Eqs. (A.18) and (A.2) imply

$$\frac{\dot{a}}{a} = H_0, \quad (\text{A.20})$$

where we have used

$$\left. \frac{dD}{dz} \right|_{z=0} = H_0^{-1}.$$

Hence the rate expansion in x -direction coincides with the measured Hubble expansion. In order to solve the system of five differential equations (Eq. (3.20) is an independent equation, since the solution $x(s)$ can also be inferred from Eq. (3.21) via the null condition), five initial conditions are needed. However, we only have two of them

$$z(0) = 0 \quad \zeta(0) = -1. \quad (\text{A.21})$$

We have two other constraints which we must satisfy at the critical point where (A.19) holds. Denoting the affine parameter at the critical point by s_{cr} , we have

$$z(s_{cr}) = z_{cr} \quad \zeta(s_{cr}) = 0. \quad (\text{A.22})$$

These lead to two other initial conditions which can be determined using the shooting method. One remaining constraint is needed and we fix it by requiring

$$\left. \frac{\dot{a}}{a} \right|_0 = \left. \frac{\dot{b}}{b} \right|_0 = H_0. \quad (\text{A.23})$$

This last condition fixes $M(0)$ and makes sure that the Hubble rate measured today is the same in any direction. We then numerically integrate the system from the critical point to the observer by varying the three remaining conditions at the critical point until the initial conditions (A.21) and (A.23) are satisfied. This matching is obtained by using the three dimensional Newton-Raphson method. Once the desired precision has been reached, the two remaining initial conditions $\beta(0)$ and $t(0)$ can simply be read from the numerical data.

B. Derivation of the system of differential equations for the redshift drift

The redshift drift for a LTB model has been derived in [26]. This approach can also be applied to our model. The null condition for the light ray (in x -direction) and the geodesic equation lead to

$$\frac{dz}{dx} = \frac{\dot{b}'}{E}(1+z), \quad \frac{dt}{dx} = -\frac{b'}{E}. \quad (\text{B.1})$$

We consider two infinitesimally close geodesics at fixed comoving position x , parametrized by

$$\{z_c, t_c\} \quad \text{and} \quad \{z_c + \delta z, t_c + \delta t\}.$$

Since the geodesic $\{z_c, t_c\}$ satisfies (B.1), it follows

$$\begin{aligned} \frac{d\delta z}{dx} &= \frac{\ddot{b}'}{E}(1+z)\delta t + \frac{\dot{b}'}{E}\delta z, \\ \frac{d\delta t}{dx} &= -\frac{\dot{b}'}{E}\delta t. \end{aligned}$$

Then, inserting (B.1) we obtain

$$\frac{d\delta z}{dz} = \frac{\ddot{b}'}{\dot{b}'}\delta t + \frac{\delta z}{1+z}, \quad (\text{B.2})$$

$$\frac{d\delta t}{dz} = -\frac{\delta t}{1+z}. \quad (\text{B.3})$$

Integrating (B.3) we find

$$\delta t = \frac{\delta t_0}{1+z}.$$

This solution together with (B.2) leads to

$$\frac{d}{dz} \left(\frac{\delta z}{\delta t_0} \right) = \frac{1}{1+z} \left(\frac{\ddot{b}'}{\dot{b}'} + \frac{\delta z}{\delta t_0} \right).$$

This equation is solved by (3.28). Deriving the Einstein equation (2.3) twice (once w.r.t. x and once w.r.t. t), we obtain

$$\ddot{b}' = \frac{2Mb'}{b^3} - \frac{M'}{b^2}. \quad (\text{B.4})$$

With (2.2) and (2.4) this results in the second line of (3.28).

C. The linearized approach

We determine the luminosity distance within linear perturbation theory for small deviations from a Friedmann–Lemaître background. Let us define

$$a(t, x) = \bar{a}(t) (1 + \epsilon f(t, x)), \quad (\text{C.1})$$

$$b(t, x) = \bar{a}(t) (1 + \epsilon g(t, x)), \quad (\text{C.2})$$

$$\rho(t, x) = \bar{\rho}(t) (1 + \epsilon \delta(t, x)), \quad (\text{C.3})$$

where the unperturbed quantities $\bar{a}(t)$, $\bar{\rho}(t)$ satisfy the Einstein equations for a flat matter dominated Friedmann universe (EdS). The perturbed quantities are determined by the Einstein equations at first order in ϵ ,

$$\frac{-6t_0^{4/3}g'' + 4t^{1/3}(\dot{f} + 2\dot{g})}{3t^{4/3}} = 8\pi G\bar{\rho}\delta, \quad (\text{C.4})$$

$$\dot{g}' = 0, \quad (\text{C.5})$$

$$t^{1/3}(2\dot{g} + t\ddot{g}) = 0, \quad (\text{C.6})$$

$$t_0^{4/3}g'' - t^{1/3}\left(2\dot{f} + 2\dot{g} + t(\ddot{f} + \ddot{g})\right) = 0. \quad (\text{C.7})$$

Neglecting the decaying mode and imposing that at the beginning the scale factors in all three directions agree, we obtain [15],

$$g = \frac{\delta_O}{3}, \quad (\text{C.8})$$

$$f = \frac{3}{10}\delta_O''t_0^{4/3}t^{2/3} + \frac{\delta_O}{3}, \quad (\text{C.9})$$

where $\delta_O(x) = \delta(t, x) + f(t, x) + 2g(t, x)$ is independent of time. This is a consequence of energy conservation and can also be derived by combining (C.4) to (C.7).

We are interested in finding the relation between δ_O and M, E in the perturbative regime. Following [16] we expand the solution (2.7, 2.8) around $\eta = 0$ in terms of $\frac{t_B(x)}{t} \ll 1$ and $\frac{E^3 t}{M} \ll 1$. Comparing the expanded solution with the linear one we find

$$M = \frac{2}{9t_0^2}(1 + \epsilon\delta_O), \quad E = \frac{\epsilon\delta_O'}{3}. \quad (\text{C.10})$$

With the ansatz (2.17, 2.19) we can identify $\delta_O(x)$ with $h(x)$ in the perturbative regime.

The angular distance is determined by Sachs focusing equation (3.6). We note that the shear term does not contribute to first order. Since light propagation is not affected by a conformal transformation, it is convenient to work with the conformally related geometry

$$ds^2 = -d\eta^2 + (1 + 2\epsilon f) dx^2 + (1 + 2\epsilon g)(dy_1^2 + dy_2^2). \quad (\text{C.11})$$

From this, we compute the Christoffel symbols (here we denote the derivative w.r.t. the conformal time η by a dot)

$$\begin{aligned} \Gamma_{11}^0 &\cong \epsilon\dot{f}, & \Gamma_{22}^0 = \Gamma_{33}^0 &\cong \epsilon\dot{g}, \\ \Gamma_{10}^1 &\cong \epsilon\dot{f}, & \Gamma_{11}^1 &\cong \epsilon f', & \Gamma_{22}^1 = \Gamma_{33}^1 &\cong -\epsilon g', \\ \Gamma_{20}^2 = \Gamma_{30}^3 &\cong \epsilon\dot{g}, & \Gamma_{21}^2 = \Gamma_{31}^3 &\cong \epsilon g', \end{aligned}$$

and the Ricci tensor

$$\begin{aligned} R_{00} &\cong -\epsilon(\ddot{f} + 2\ddot{g}), \\ R_{10} &\cong -2\epsilon\dot{g}', \\ R_{11} &\cong \epsilon(\ddot{f} - 2g''), \\ R_{22} = R_{33} &\cong \epsilon(\ddot{g} - g''). \end{aligned}$$

At 0-order we are free to parametrize the affine parameter s such that $\bar{n}^0 = 1$ and $\bar{n}^i = \delta^{i1}$ (we are interested in the distance in x -direction). With this we obtain the coefficient \mathcal{R}

$$\mathcal{R} = -\epsilon (\ddot{g} + g'' + 2\dot{g}').$$

Consistently with the parametrization of the affine parameter s such that $n^0(s_o) = 1$, the initial conditions are $D(s_o) = 0$ and $D'(s_o) = -1$. After an integration by parts we find the solution to Sachs focusing equation (3.6),

$$D(s) = (s_o - s)(1 + \epsilon g(s_o) + \epsilon g(s)) + 2 \int_{s_o}^s ds' \epsilon g(s'). \quad (\text{C.12})$$

With the above initial conditions for the Sachs focusing equation, we consider a thin light bundle with the vertex at the observer position. Hence the solution (C.12) is the angular diameter distance, see [23]. To determine the luminosity distance we have to compute also the redshift, using the geodesic equation for n^0 ,

$$1 + z = \frac{g_{\mu\nu} n^\mu u^\nu|_e}{g_{\mu\nu} n^\mu u^\nu|_o} = n^0|_e = 1 - \int_{s_o}^{s_e} ds \epsilon \dot{f}, \quad (\text{C.13})$$

where $|_e$ denotes the emission point, the source, and we denote the affine parameter at the source by s_e . With the same geodesic equation we derive the relation between the conformal time η and the affine parameter s , $n^0 = d\eta/ds$,

$$\eta_o - \eta_e = s_o - s_e + \int_{s_o}^{s_e} ds \int_{s_o}^s ds' \epsilon \dot{f}(s'). \quad (\text{C.14})$$

In terms of conformal time the luminosity distance then becomes

$$D_L(\eta_e) = (\eta_o - \eta_e) \left(1 + \epsilon g_o + \epsilon g_e - 2 \int_{\eta_o}^{\eta_e} d\eta \epsilon \dot{f} \right) + 2 \int_{\eta_o}^{\eta_e} d\eta \epsilon g - \int_{\eta_o}^{\eta_e} d\eta \int_{\eta_o}^{\eta} d\eta' \epsilon \dot{f}. \quad (\text{C.15})$$

All of this is valid in the conformal geometry, where the expansion of the Universe is divided out. Taking into account the expansion of the universe, changes the relation between the affine parameter and conformal time. The luminosity distance scales as [6]

$$\tilde{D}_L = \frac{\bar{a}^2(\eta_o)}{\bar{a}(\eta_e)} D_L = \frac{D_L}{\bar{a}(\eta_e)} = (1 + \bar{z}_e) D_L.$$

Since conformal time is not an observable quantity, we rewrite the distance in term of the observed redshift. We define the observed redshift as $z_e = \bar{z}_e + \delta z_e$ and we compute the correction term. The same calculation as presented in Ref. [6] leads to

$$\left(\frac{d}{dz} \tilde{D}_L \right) \delta z_e = ((\eta_o - \eta_e) + \mathcal{H}_e^{-1}) \delta z_e, \quad (\text{C.16})$$

where

$$\delta z_e = -(1 + z_e) \int_{\eta_o}^{\eta_e} d\eta \epsilon \dot{f}. \quad (\text{C.17})$$

Subtracting (C.16) we obtain the distance–redshift relation

$$\begin{aligned} \tilde{D}_L(z_e) &= (1+z_e)(\eta_o - \eta_e) \left(1 + \epsilon g_o + \epsilon g_e - \int_{\eta_o}^{\eta_e} d\eta \epsilon \dot{f} \right) \\ &+ (1+z_e) \left(2 \int_{\eta_o}^{\eta_e} d\eta \epsilon g - \int_{\eta_o}^{\eta_e} d\eta \int_{\eta_o}^{\eta} d\eta' \epsilon \dot{f} \right) + \frac{1+z_e}{\mathcal{H}_e} \int_{\eta_o}^{\eta_e} d\eta \epsilon \dot{f}. \end{aligned} \quad (\text{C.18})$$

With

$$- \int_{\eta_o}^{\eta_e} d\eta \int_{\eta_o}^{\eta} d\eta' \epsilon \dot{f} = (\eta_e - \eta_o) \int_{\eta_e}^{\eta_o} d\eta \epsilon \dot{f} + \int_{\eta_e}^{\eta_o} d\eta \int_{\eta_e}^{\eta} d\eta' \epsilon \dot{f},$$

we can rewrite the above expression in the form as

$$\begin{aligned} \tilde{D}_L(z_e) &= (1+z_e)(\eta_o - \eta_e) (1 + \epsilon g_o + \epsilon g_e) \\ &+ (1+z_e) \left(-2 \int_{\eta_e}^{\eta_o} d\eta \epsilon g + \int_{\eta_e}^{\eta_o} d\eta \int_{\eta_e}^{\eta} d\eta' \epsilon \dot{f} \right) - \frac{1+z_e}{\mathcal{H}_e} \int_{\eta_e}^{\eta_o} d\eta \epsilon \dot{f}. \end{aligned} \quad (\text{C.19})$$

Using the solutions (C.8, C.9) we express the distance in terms of $\delta_O(\eta)$. Conformal time is defined as

$$d\eta = \frac{dt}{\bar{a}(t)} \Rightarrow \eta(t) = 3t^{1/3}t_0^{2/3}, \text{ setting } \eta(0) = 0.$$

This leads to

$$\begin{aligned} g(\eta, x(\eta)) &= \frac{\delta_O(x(\eta))}{3}, \\ f(\eta, x(\eta)) &= \frac{1}{30} \delta_O''(x(\eta)) \eta^2 + \frac{\delta_O(x(\eta))}{3}, \\ \dot{f}(\eta, x(\eta)) &= \frac{1}{15} \delta_O''(x(\eta)) \eta, \end{aligned}$$

and consequently to the following distance–redshift relation

$$\begin{aligned} D_L(z_e) &= (1+z_e)(\eta_o - \eta_e) \left(1 + \frac{\epsilon}{3} (\delta_O(x(\eta_o)) + \delta_O(x(\eta_e))) \right) - (1+z_e) \int_{\eta_e}^{\eta_o} \frac{2\epsilon}{3} \delta_O(x(\eta)) d\eta \\ &+ (1+z_e) \int_{\eta_e}^{\eta_o} d\eta \int_{\eta_e}^{\eta} d\eta' \frac{\epsilon}{15} \delta_O''(x(\eta')) \eta' - \frac{1+z_e}{\mathcal{H}_e} \int_{\eta_e}^{\eta_o} d\eta \frac{\epsilon}{15} \delta_O''(x(\eta)) \eta. \end{aligned} \quad (\text{C.20})$$

References

- [1] A. Riess et al. *Astron. J.* **116**, 1009 (1998) [arXiv:astro-ph/9805201v1];
S. Perlmutter et al., *Astrophys. J.* **517**, 565 (1999) [arXiv:astro-ph/9812133v1].
- [2] R. Amanullah et al., *Astrophys. J.* **716**, 712 (2010) [arXiv:1004.1711v1];
J. Guy et al. (2010), arXiv:1010.4743v1;
T. Holsclaw, et al., *Phys. Rev. Lett.* **105**, 241302 (2010) [arXiv:1011.3079v1];
N. Suzuki et al. (2011), arXiv:1105.3470v1.
- [3] J. Dunkley et al., *Astrophys. J.* **739**, 52 (2011) [arXiv:1009.0866].

- [4] R. Durrer, Phil. Trans. R. Soc. A **369**, 5102 (2011), doi: 10.1098/rsta.2011.0285 [arXiv:1103.5331].
- [5] C. Blake et al., Mon. Not. Roy. Ast. Soc. **418**, 1725 (2011) [arXiv:1108.2637].
- [6] C. Bonvin, R. Durrer and A. Gasparini, Phys. Rev. D **73**, 023523 (2006) [arXiv:astro-ph/0511183v4].
- [7] C. Vale and M. White, Astrophys. J. **592**, 699 (2003) [arXiv:astro-ph/0303555v1];
K. Kainulainen and V. Marra, Phys. Rev. D **83**, 023009 (2011) [arXiv:1011.0732].
- [8] S. Räsänen, Class. Quant. Gravity **28**, 164008 (2011) [arXiv:1102.0408].
- [9] G. Lemaître, 1933 Ann. Soc. Sci. Bruxelles **A 53**, 51 (1933); (English translation, with historical comments: Gen. Rel. Grav. **29** 637, 1997).
- [10] R.C. Tolman, Proc. Nat. Acad. Sci. USA **20**, 169 (1934); (reprinted, with historical comments: Gen. Rel. Grav. **29** 931, 1997).
- [11] For recent overviews see:
K. Bolejko, M-N. Célérier and A. Krasinski, Class. Quantum Grav. **28**, 164002 (2011) [arXiv:1102.1449v2];
V. Marra and A. Notari, Class. Quantum Grav. **28**, 164004 (2011) [arXiv:1102.1015].
- [12] P. Szekeres, Com. Math. Phys. **41**, 55 (1975); Phys. Rev. D **12**, 2941 (1975).
- [13] A. Krasinski and K. Bolejko, Phys. Rev. D **83**, 083503 (2011), [arXiv:1007.2083v2].
- [14] N. Meures and M. Bruni, MNRAS **419**, 1937 (2012) [arXiv:1107.4433v2] (DOI: 10.1111/j.1365-2966.2011.19850.x).
- [15] H. Collins (2010), arXiv:1011.2046v1.
- [16] A. V. Zakharov, Soviet Physics Journal **30**, 1015 (1987).
- [17] J. Plebanski and A. Krasinski, *An Introduction to General Relativity and Cosmology*, (Cambridge, 2006).
- [18] C.-M. Yoo, T. Kai, K. Nakao, Prog. Theor. Phys. **120**, 937 (2008) [arXiv:0807.0932].
- [19] E. Komatsu et al., ApJS, **192**, 18, (2011) [arXiv:1001.4538v3].
- [20] H. El-Ad and T. Piran, ApJ, **491**, 421(1997) [arXiv:astro-ph/9702135v1].
- [21] P. Schneider, J. Ehlers and E.E. Falco, *Gravitational Lenses*, (Springer Verlag, 1992).
- [22] N. Straumann, *General Relativity with Applications to Astrophysics*, (Springer Verlag, 2004).
- [23] S. Seitz, P. Schneider and J. Ehlers, Class. Quantum Grav. **11**, 2345 (1994) [arXiv:astro-ph/9403056v1].
- [24] V. Marra, E. W. Kolb, S. Matarrese and A. Riotto, Phys. Rev. D **76**, 123004 (2007) [arXiv:0708.3622v3].
- [25] Philip Bull, Timothy Clifton, Pedro G. Ferreira, arXiv:1108.2222 (2011).
- [26] C.-M. Yoo, T. Kai, K. Nakao, Phys. Rev. D **83**, 043527 (2011) [arXiv:1010.0091].
- [27] V. Perlick, Living Reviews in Relativity, **7**, 9 (2004).